metals

MDPI

Article

Influence of In Situ Magnetic Field on Magnetic Properties of a Bonded Permanent Magnet Manufactured through Material Extrusion Additive Manufacturing

Ji Yong Hwang [1], Seong Je Park [2], Yong Son [1] and Hyo Yun Jung [1,*]

[1] Additive Manufacturing Innovation Agency, Korea Institute of Industrial Technology (KITECH), 113-58 Seohaean-ro, Siheung 15014, Republic of Korea; hwangjy@kitech.re.kr (J.Y.H.); sonyong@kitech.re.kr (Y.S.)
[2] School of Mechanical and Aerospace Engineering, Nanyang Technology (NTU), 50 Nanyang Avenue, Singapore 639798, Singapore; seongje.park@ntu.edu.sg
* Correspondence: hjung@kitech.re.kr

Abstract: In this study, a material extrusion (MEX) nozzle for fabricating bond magnets was designed to form a unidirectional magnetic field with a solenoid. The hard magnetic properties of the bonded magnets were enhanced by induced magnetic anisotropy. The magnetic field strength for magnetic alignment was controlled by the current applied to the solenoid, and the magnetic field strength formed at the bottom of the solenoid was approximately 10 mT. When a magnetic field was applied to the magnetic particles in filaments, magnetic spins and domains that existed in spherical magnetic particles were magnetically rotated and preferentially aligned with the induced magnetic field. Subsequently, as the polymer matrix was softened by the heat generated by the current induced in the solenoid, bonded magnets were additively manufactured using MEX with in situ magnetic field, and hard magnetic properties such as coercivity, remanence, and maximum energy product of the manufactured magnets were confirmed to be enhanced. The improvement in hard magnetic properties was attributed to the increased magnetic anisotropy caused by magnetic alignment. Based on the results of this study, we expect MEX with a magnetic field application system to be used in the future for manufacturing complex-shaped bonded magnets with improved magnetic properties.

Keywords: material extrusion; in situ magnetic alignment; bonded permanent magnet; magnetic field application system; solenoid

check for updates

Citation: Hwang, J.Y.; Park, S.J.; Son, Y.; Jung, H.Y. Influence of In Situ Magnetic Field on Magnetic Properties of a Bonded Permanent Magnet Manufactured through Material Extrusion Additive Manufacturing. *Metals* **2023**, *13*, 1653. https://doi.org/10.3390/met13101653

Academic Editor: Chun Guo

Received: 5 September 2023
Revised: 23 September 2023
Accepted: 25 September 2023
Published: 27 September 2023

1. Introduction

Nd-Fe-B bonded magnets are widely used in fields such as robotics and for producing smart appliances and eco-friendly automobiles. With the expansion of the electronics business for hybrid and electric vehicles owing to environmental issues, the demand for Nd-Fe-B bonded magnets is expected to grow [1–3]. Bonded magnets are typically manufactured using injection and compression molding with polymer binders [4–6]. Thus far, bonded magnets have been manufactured by rapidly injecting materials into a mold with a certain shape or through pressure molding, which requires the use of a mold. The use of molds limits the shape of bonded magnets, and changing the shape of bonded magnets requires the production of new molds, which is a disadvantage.

To overcome these problems, additive manufacturing (AM), which mainly uses material extrusion (MEX) with feedstock composed of magnet powder and a polymer binder in the form of filaments or pellets, has been applied recently [1,7–11]. The manufacturing of bonded magnets using MEX, first proposed by Huber et al. [12], involves softening the thermoplastic binder of the feedstock by heating the MEX nozzle, then directly manufacturing bonded magnets by stacking the softened material in three dimensions (3D) on a build plate. The technology for manufacturing bonded magnets using MEX has the advantage

of being able to produce complex-shaped bonded magnets without molds. By manufacturing complex-shaped bonded magnets without molds, machining can be minimized, simplifying the process and reducing manufacturing costs. When comparing MEX to other additive manufacturing processes, i.e., powder bed fusion, direct energy deposition, and binder jetting, MEX is cost-effective because it does not require expensive energy beams and nozzles, enabling economical production in terms of initial equipment investment and 3D product manufacturing. Moreover, the operation and handling of feedstock in MEX are simple and easy, compared to other AM processes using powder-type feedstocks. Thus, MEX has garnered significant attention. With the recent difficulties in securing rare earth elements contained in Nd-Fe-B materials, as well as price instability, the efficient use of Nd-Fe-B materials in AM technology has substantial advantages in the manufacturing of bonded magnets [7,13,14].

Bonded magnets consist of a polymer binder and magnet powder. Owing to the non-magnetism of the binder, the magnet powder content is inevitably reduced and the magnet powder is isolated, which can lead to a decrease in magnetic properties. Therefore, by introducing magnetic anisotropy to the magnet powder, hard magnetic properties of the bond magnet, particularly remanence, coercivity, and maximum energy product (BH_{max}), have been improved. In conventional manufacturing processes, the remanence and coercivity of the bond magnet are increased by introducing magnetic anisotropy through magnetic annealing or magnetic alignment, thus improving BH_{max} [5,6,15–17]. Regarding the development of AM-bonded magnets, Gandha et al. [18] investigated the effectiveness of post-printing magnetic alignment at various temperatures and magnetic fields, and they confirmed that hard magnetic properties in MEX-bonded magnets were improved. This improvement in hard magnetic properties demonstrates that despite the relatively low magnet powder content of bonded magnets, it is effective in maximizing magnetic properties.

Suppan et al. [19] demonstrated the effect of in situ magnetic alignment through 3D printing using MEX in an external magnetic field formed by permanent magnets, and Sarkar et al. [20] proposed a mechanistic multiphysics model for predicting the degree of magnetic alignment. However, in recent studies, permanent magnets were mostly installed at the nozzle to form an external magnetic field, and the magnetic field strength was controlled by replacing the permanent magnets or adjusting the physical distance between the permanent magnets and the nozzle [18,19,21,22]. When using permanent magnets to form an external magnetic field, the temperature increase around the permanent magnets, due to the heat applied to the nozzle to extrude feedstock, causes a decrease in the magnetic force applied to the nozzle side. Therefore, magnetic field application based on electromagnetic induction is required to properly apply magnetic fields, but research and consideration on the design and application of a nozzle for an in situ magnetic field application are insufficient.

This study investigates the MEX printing method, which applies a magnetic field using electromagnetic induction. MEX with a magnetic field application system based on electromagnetic induction was designed to induce magnetic anisotropy during the fabrication of the bonded magnet, and it examined the effect of in situ magnetic alignment on magnetic properties. This method makes it possible to manufacture magnetically aligned bonded magnets in a single process; thus, not only does it improve the shape freedom, but it also simplifies the process. Furthermore, applying magnetic fields during the 3D manufacturing process can develop the anisotropy of magnetic properties by tailoring the degree and direction of magnetization, and can also characterize the magnetic properties.

2. Materials and Methods

The MEX nozzle was designed to form in situ magnetic field with a solenoid. The manufacturing process conditions for the bonded magnet were investigated using the designed MEX nozzle and composite filament. Bulk bonded magnets were manufactured

under selected printing conditions while applying the magnetic fields, and changes in magnetic properties due to in situ magnetic alignment were examined.

2.1. Nozzle with a Magnetic Field Application System

Figure 1 shows a schematic of the MEX printer nozzle used in this study, which was equipped with a solenoid to apply a magnetic field during the melting and extrusion of the composite filament, as well as to control the strength of the formed magnetic field [23].

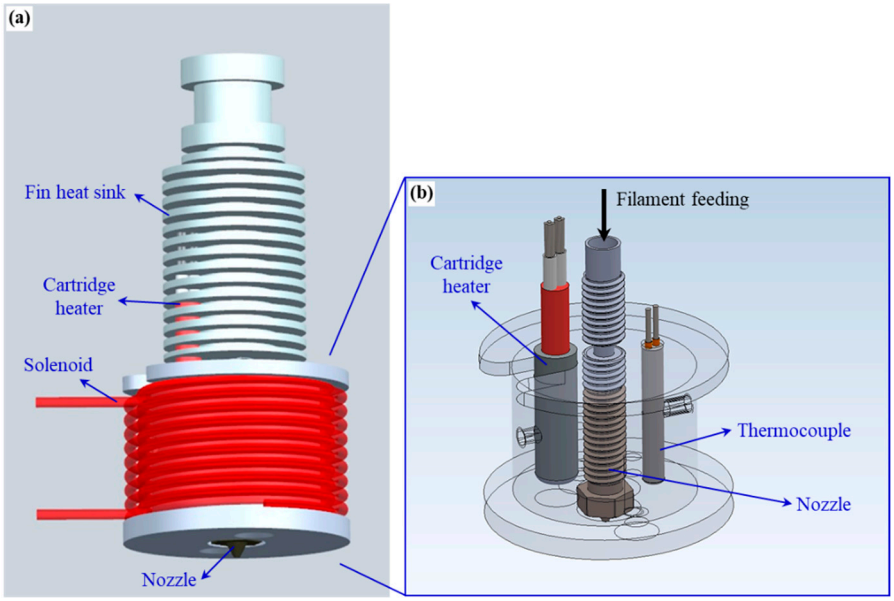

Figure 1. Schematics of (**a**) nozzle equipped with a solenoid and (**b**) heating part of nozzle.

The magnetic field strength was adjusted by controlling the applied current. A cartridge heater and thermocouple were also installed in the nozzle part for heating the filament and monitoring its temperature, respectively (Figure 1b). By applying a magnetic field using the current flowing through the solenoid and heating the filament to the required temperature using the cartridge heater, the polymer binder was softened, enabling the alignment of the magnet powder and extrusion of the filament.

Figure 2a shows an extruder with a solenoid-equipped nozzle. The extruder used in a previous study consisted of a heating block and a nozzle, with a short melting zone range of 10 mm [24]. In comparison, the melting zone of the extruder used in this study was extended to 20 mm with the solenoid positioned in the melting zone to build a magnetic field formation system (Figure 2b). In previous studies, shorter melting zones were adopted to avoid unsteady viscoelastic flow causing instability in extruded strands. However, in this study, a longer range of applied magnetic fields was required to enhance the magnetic alignment effect. The extruder's melting zone length of 20 mm and the solenoid's continuous application throughout this length were, therefore, intended to increase the efficacy of magnetic alignment. In this case, magnetic field control and thermal process variables, such as nozzle and chamber temperatures, were crucial factors for setting stable printing conditions of the magnetic filament.

To induce a magnetic field around the magnetic filament, current flows through the solenoid. The magnetic field strength can be controlled by adjusting the current. The magnetic field formed by the solenoid can be calculated theoretically using Ampere's law, defined by Equations (1) and (2) depending on the position where the magnetic field is measured. Figure 3a,b illustrate the positions where the magnetic field is calculated.

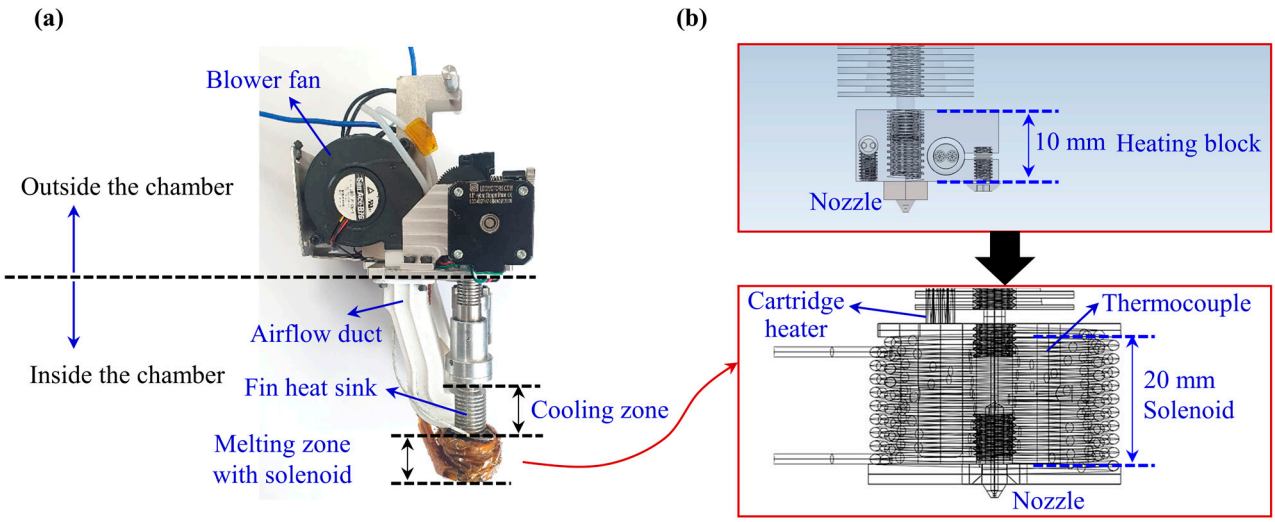

Figure 2. (**a**) Extruder with the nozzle part equipped with in situ magnetic field application system and (**b**) comparison of the nozzle part with that of the previous extruder [24].

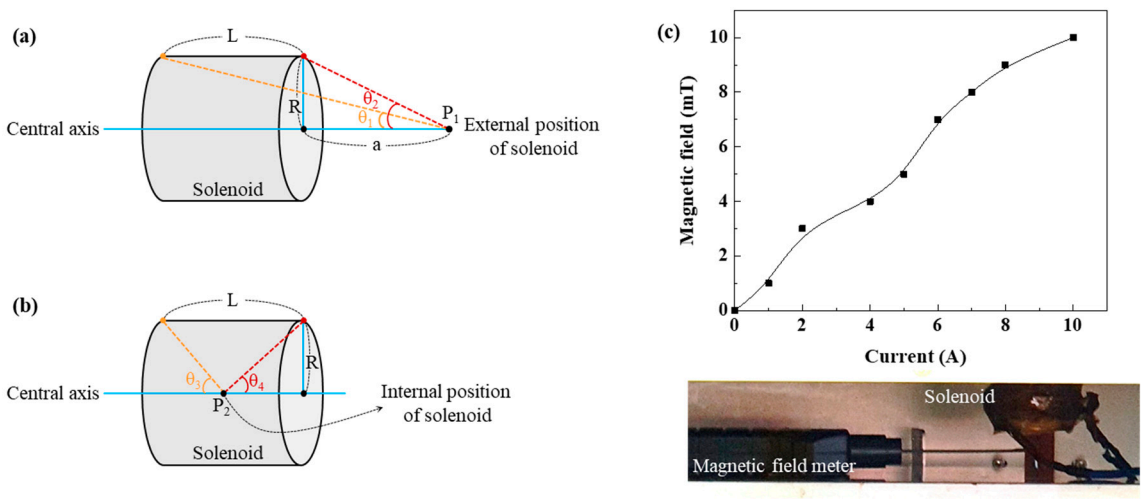

Figure 3. Schematics of the theoretical calculations of the magnetic field strength at the (**a**) external point and (**b**) internal point of the solenoid. (**c**) Measurement results of the magnetic field formed in the nozzle with in situ magnetic field application, and an image of the measurement method.

The magnetic field at an external point P1 on the solenoid's central axis is given by (Figure 3a):

$$B = \frac{\mu_0}{2} nI \left\{ \frac{a+L}{\sqrt{R^2+(a+L)^2}} - \frac{a}{\sqrt{R^2+a^2}} \right\} = \frac{\mu_0}{2} nI(\cos\theta_1 - \cos\theta_2) \quad (1)$$

The magnetic field at an internal point P2 on the solenoid's central axis is expressed as (Figure 3b):

$$B = \frac{\mu_0}{2} nI(\cos\theta_3 + \cos\theta_4) \quad (2)$$

where B denotes the magnetic field (T), μ_0 denotes the vacuum permeability ($4\pi \times 10^{-7}$, T·m·A^{-1}), n denotes the number of turns per unit length (turns/m), I denotes the current (A), R denotes the solenoid radius (m), a denotes the distance from the solenoid to the external point (m), L denotes the solenoid length (m), and θ denotes the angle between the specified position and the end of the solenoid (degrees).

The magnetic field strength formed in the nozzle was measured using an AC/DC magnetic field meter. In Figure 3c, the magnetic field strength measured in the in situ magnetic field-applied nozzle is presented as a function of current. The results show that the magnetic field strength increased linearly with increasing current and reached a maximum of 10 mT at 10 A. The solenoid used in this study was wound with enamel wire (Ø1.02 mm) for 47 turns, with an average diameter of 29 mm and a winding length of 20 mm. The in situ magnetic field formation using a solenoid was found to be effective, as there was no difference in the magnetic field strength when the nozzle (~310 °C) and chamber (80 °C) were heated. Considering the applied current of 10 A and the same position as the actual measurement, the calculated magnetic field strength was 11.08 mT according to Equation (1), and the result showed good agreement with a small error of approximately 1 mT from the actual measurement value. Meanwhile, the magnetic field strength, determined using Equation (2), was 16.57 mT at the center point inside the solenoid. Considering the error similar to the aforementioned one, the actual magnetic field strength formed at the center point inside the solenoid was estimated to be approximately 15 mT.

2.2. MEX Process and Property Analysis

The feedstock used in this study was a composite filament consisting of Nd-Fe-B magnet powder and PA12 polymer binder (Figure 4). The composite filament was developed in-house by extruding a mixture of the Nd-Fe-B powder and binder at a volume ratio of approximately 30:70. Mixing was performed three times to uniformly disperse the magnet powders. The Nd-Fe-B powder was a hard magnet powder (Magnequench, MQP-S-11-9-20001-070, Singapore) produced through gas atomization, and it had a spherical shape (Figure 4a). To reduce the viscosity of the mixture and increase its flexibility, small amounts of stearic acid and paraffin wax were used as additives. The filament was produced with a certain diameter (1.65 ± 0.3 mm) and uniform appearance (Figure 4b,c). In the filaments, the magnetic particles were evenly distributed in the binder matrix, and pores were partially confirmed (Figure 4d,e). Permanent magnets were manufactured using the composite filament.

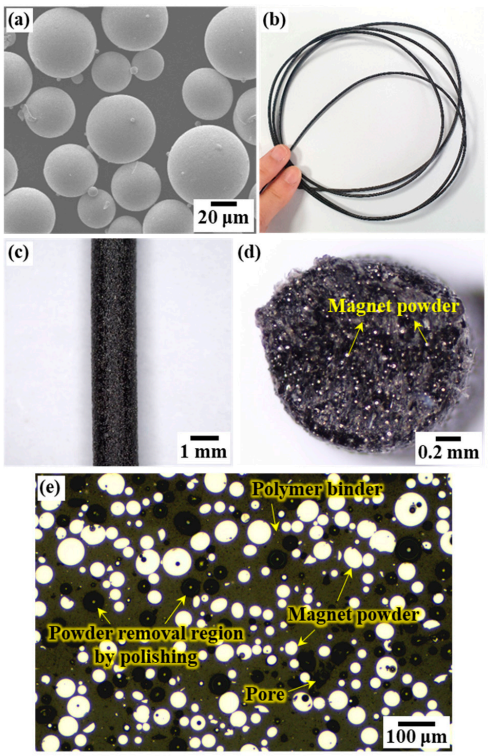

Figure 4. (**a**) Nd-Fe-B magnet powder used for the composite filament; (**b**,**c**) appearance and (**d**,**e**) cross-section of the self-developed composite filament.

To avoid the occurrence of deformation during printing, the entire chamber was preheated to 80 °C. The chamber temperature was maintained at the set value for approximately 1 h to minimize temperature variations inside the chamber. Printing was performed in a chamber preheated at 80 °C, despite the glass transition temperature of the used PA12 being 130 °C. The heat-shrinkage prevention effect of the powder contained in the filament helped to ensure dimensional stability during printing. Samples were produced more than three times under each printing condition with controlled nozzle temperature and scan speed, and the reproducibility was confirmed by examining the microstructure and external shape of the sample. The printing conditions are outlined in Table 1.

Table 1. MEX processing conditions.

Nozzle Temperature (°C)	260–310
Flow rate (mm^3/s)	3.6–11.1
Printing speed (mm/s)	2–10
Magnetic field (mT)	0, 10
Layer thickness (mm)	0.2
Scan pattern	Zigzag pattern

To ensure the shape of the bonded magnets, printing conditions were optimized based on the surface roughness (R_a) measurements of the produced 3D-shaped samples. The surface roughness was measured using a surface roughness tester (Mitutoyo, SJ-410, Kawasaki, Japan) according to ISO 1997, and an average of five measurements per sample was taken. The surface morphology was observed through optical microscopy (OM, ZEISS, Stemi 508, Oberkochen, Germany) and field emission scanning electron microscopy (FE-SEM, FEI Hong Kong Company, NNS-450, Hong Kong, China). Hardness measurements were performed using the Rockwell R method according to ASTM D785 (Mitutoyo, HR-500, Kawasaki City, Japan), and the average value was obtained from 10 measurements. Samples for the hardness test were manufactured under selected printing conditions and prepared through polishing. Bonded magnet samples for the magnetic property analysis were produced under the optimized printing conditions with varying magnetic field strengths. Certain produced samples were cut to approximately 5 × 5 × 6 mm for magnetic property evaluation. The magnetic properties of the produced samples were analyzed using vibrating sample magnetometers (Lakeshore Cryotronics, 7407-S, Westerville, OH, USA), in which a ±18 kOe magnetic field was applied. The analysis included measurements of magnetic properties such as remanence, coercivity, and BH_{max}, which are important factors in determining the performance of bonded magnets.

3. Results and Discussion

3.1. Fabrication of the Bonded Magnet

The fabrication of two types of bonded magnets with varying heights (15 × 15 × 2 mm and 15 × 15 × 6 mm) using the MEX nozzle with the in situ magnetic field application system was performed under controlled printing conditions. The surface morphology of the fabricated samples was observed to analyze the effect of the applied magnetic field and printing parameters. Surface observation images of 2 mm height samples fabricated at different nozzle temperatures and the same flow rate (8.8 mm^3/s) are presented in Figure 5, along with shape differences of the samples shown in Table 2. As shown in Figure 5, an increase in protrusions on the sample surface is observed as the nozzle temperature increases above 290 °C owing to an overflow caused by the decrease in the binder viscosity and increase in fluidity (indicated by arrows). This increase in protrusions leads to a higher R_a value of samples produced at temperatures above 290 °C, resulting in a deterioration of the surface roughness of the sample and making it more prone to forming stacking defects in the next layer. In contrast, at nozzle temperatures of 270–280 °C, no protrusions

were observed, and a healthy surface formation was demonstrated. At temperatures below 260 °C, the weak adhesion between the build plate and printed layer resulted in an incomplete printing process, failing to achieve the intended 3D shape owing to the warpage of printed layers. Given that magnetic materials lose their magnetic properties when heated above their Curie temperature (which is 320 °C in this case), a nozzle temperature of 280 °C was selected to ensure stable extrusion without affecting the magnetic properties of the particles.

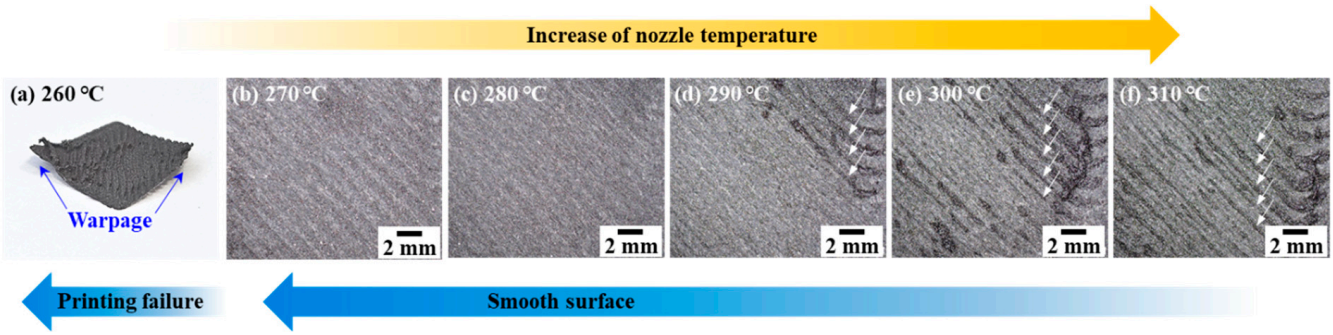

Figure 5. Surface morphology of as-printed samples at different nozzle temperatures under the same flow rate (8.8 mm^3/s): (**a**) 260, (**b**) 270, (**c**) 280, (**d**) 290, (**e**) 300, and (**f**) 310 °C.

Table 2. Comparison of morphology of as-printed samples at different nozzle temperatures under the same flow rate (8.8 mm^3/s). Indication of the relative state/morphology of as-printed samples: X (none), △ (moderate), ○ (severe).

	Nozzle Temp. (°C)					
	260	**270**	**280**	**290**	**300**	**310**
Protrusion by overflow	-	X	X	△	○	○
Surface hole	-	X	X	X	X	X
Adhesion to the build plate	weak	weak	good	good	good	good
Warpage	○	△	X	X	X	X
Roughness, Ra (μm)	-	8.62	10.21	18.97	34.80	38.06

With the nozzle temperature fixed at 280 °C, the flow rate was adjusted to produce samples without surface defects, such as holes and protrusions, and the shape changes of the samples were examined, as shown in Figure 6. The characteristics of the samples produced for each flow rate are summarized in Table 3. As shown in Figure 6c–e, excess molten filament lumps were formed owing to overflow at the edge (indicated by circles) at flow rates of 7.2 mm^3/s and above, and the intended shape could not be properly realized because of these lumps. Surface defects such as holes and protrusions were also observed. As the flow rate decreased (Figure 6a,b), the samples showed relatively clean edge shapes, but holes smaller than 1 mm began to appear, as shown in Figure 6b, and the number and size of holes tended to increase with further decreases in flow rate (Figure 6a) owing to insufficient extrusion. Therefore, to improve the surface roughness, the flow rate was adjusted between 5.8 and 7.2 mm^3/s, considering that the sample in Figure 6b possessed the lowest surface roughness (8.94 μm).

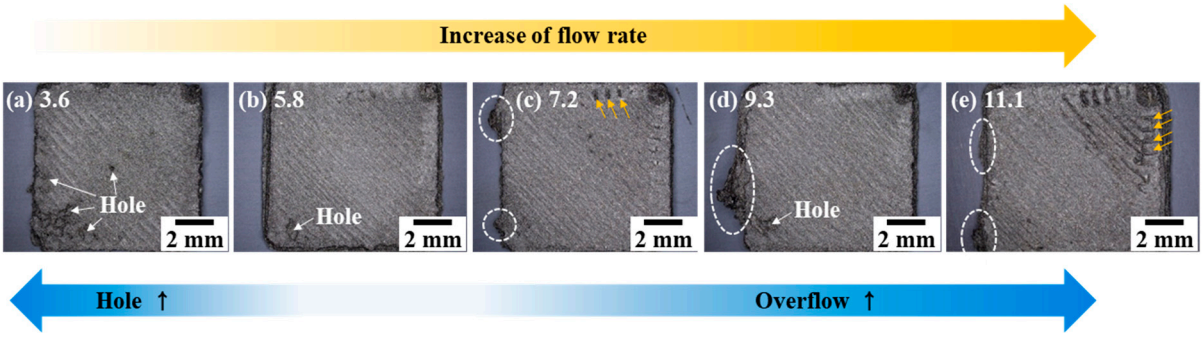

Figure 6. Morphologies of as-printed samples according to the flow rate at a nozzle temperature of 280 °C: (**a**) 3.6, (**b**) 5.8, (**c**) 7.2, (**d**) 9.3, and (**e**) 11.1 mm^3/s.

Table 3. Comparison of morphologies of as-printed samples according to the flow rate at a nozzle temperature of 280 °C. Indication of the relative state/morphology of as-printed samples: X (none), △ (moderate), ○ (severe).

	Flow Rate (mm^3/s)				
	3.6	**5.8**	**7.2**	**9.3**	**11.1**
Protrusion by overflow	X	X	△	X	○
Surface hole	○	△	X	△	X
Adhesion to the build plate	good	good	good	good	good
Warpage	X	X	X	X	X
Roughness, Ra (μm)	10.36	8.94	12.38	10.21	20.84

Figure 7 illustrates a bulk sample produced under the aforementioned conditions. The sample was printed with dimensions of 15 × 15 × 6 mm, and the actual measured width and length were 15.38 ± 0.04 mm, while the height was 5.90 ± 0.02 mm, exhibiting an error of approximately 2–3%, compared to the design dimensions. The relative density was 93% of the theoretical density of the filament (3.05 g/cm^3), which corresponds to approximately 2.84 g/cm^3, accounting for a decrease in the density caused by initial pores in the filament. Notably, as depicted in Figure 7b–e, magnetic particles embedded in the binder matrix and extrusion-induced open pores were observed on the surface, and the evenly dispersed magnetic particles were confirmed in the cross-section. Regarding changes in the distribution of magnetic particles under a magnetic field, Sonnleitner et al. [21] reported that when a bonded magnet with magnetic particles of approximately 5 μm in size was manufactured under a magnetic field of approximately 550 mT, the magnetic particles exhibited a distribution aligned parallel to the external magnetic field. In the case of a bonded magnet including magnetic particles larger than ~150 μm [18], the parallel distribution of the magnetic particles was confirmed in post-magnetic aligned samples applying a strong magnetic field (1500 mT). In this study, a bulk sample composed of magnetic particles with an average diameter of 50 μm was manufactured under a magnetic field of approximately 10~15 mT. The magnetic field applied in this study was not strong enough to change the distribution of magnetic particles; thus, the magnetic particles were uniformly distributed. However, the applied magnetic field can have the effect of increasing magnetic anisotropy, as will be discussed in the magnetic analysis results. Average hardness values of the bulk sample were 61.6 ± 0.8 HRR. The top surface's average roughness was 7.93 μm, indicating an improvement by adjusting the flow rate, compared to the results summarized in Table 3. In addition, Figure 7f displays a segment magnet produced under the same conditions. The segment magnet had a width of 6.05 ± 0.2 mm, height of 5.89 ± 0.05 mm, and density of approximately 2.87 g/cm^3. The average surface roughness

and Rockwell hardness of the segment magnet were 7.41 μm and 60.2 ± 0.9 HRR, exhibiting an error of approximately 2–4% compared to the design dimensions. Thus, the surface characteristics of the segment magnet were comparable to those of the block magnet.

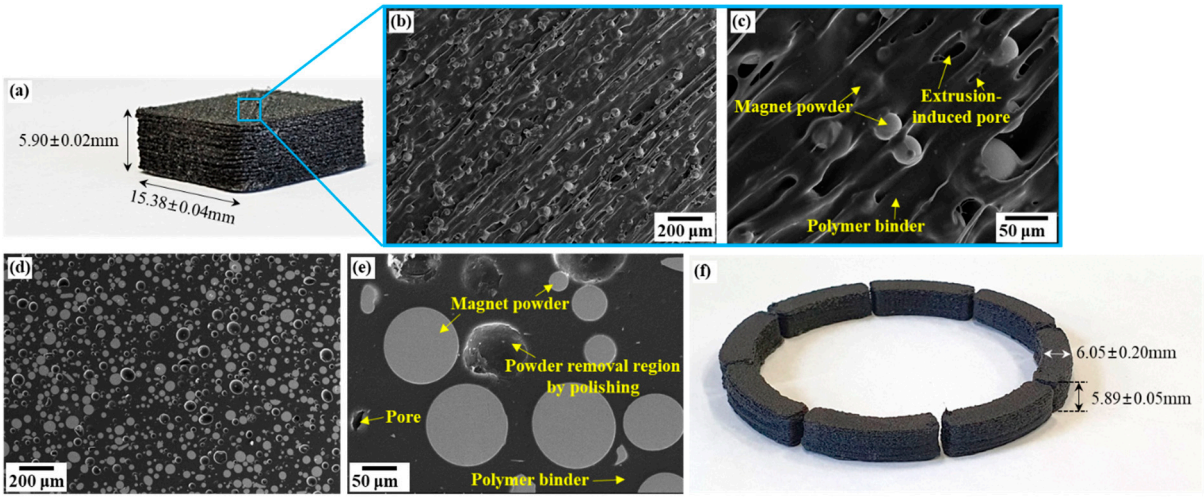

Figure 7. (**a**) Bulk sample fabricated under selected conditions. (**b**,**c**) Top surface and (**d**,**e**) cross-section of the bulk sample. (**f**) Segment magnet.

3.2. Magnetic Properties of MEX-Manufactured Bonded Magnets with In Situ Magnetic Field Application

Figure 8 illustrates the magnetic alignment process of magnetic particles under an induced magnetic field during MEX, along with the main magnetic alignment direction of the as-printed samples. As depicted in Figure 8a, the solenoid generates a magnetic field in the direction of the red arrows when current is applied. The magnetic torque caused by the magnetic field causes the rotation and alignment of magnetic spins and domains in magnetic particles, aligning their magnetization direction (blue arrow) to the magnetic field direction [19]. This results in magnetic alignment in the perpendicular direction of the build plate, increasing the magnetic anisotropy (Figure 8b). Magnetic property analysis was performed by applying an external magnetic field parallel to the induced magnetic alignment direction of the samples. Table 4 summarizes the analysis results of the magnetic properties while Figure 8c shows the magnetic hysteresis curve with and without magnetic field application. The application of a 10 mT magnetic field during printing led to an increase in the ratio of remanence to saturation magnetization (M_r/M_s) and the slope of the initial magnetization curve. The value of M_r/M_s represents the squareness of the magnetic hysteresis curve and depends on the angle between the external magnetic field direction and the easy axis of magnetization. A value closer to one indicates a more square-shaped hysteresis curve, which is achieved when the external magnetic field direction is parallel to the easy axis of magnetization. Thus, an increase in M_r/M_s indicates an improvement in the magnetic alignment of the magnetic particles. The initial magnetization curve illustrates the magnetization behavior as the external magnetic field increases. As the external magnetic field aligns with the easy axis of magnetization, magnetization occurs more rapidly, resulting in an increase in the slope of the initial magnetization curve, indicating improved magnetic alignment. The samples with magnetic field application exhibited relatively higher values of coercivity and BH_{max}. Coercivity refers to the strength of the reverse magnetic field required to make magnetization zero, and it depends on two demagnetization processes [16]. These processes can be affected by the printing temperature, strength of the applied magnetic field, and size of magnetic particles [25,26]. The two demagnetization processes exhibit opposite tendencies to increase or decrease coercivity depending on magnetic alignment. Because coercivity arises because of the complex interaction of the two opposing demagnetization processes, it shows weak dependence on the degree of magnetic alignment. Meanwhile, BH_{max} represents the

maximum energy that a permanent magnet can supply, and its increase is related to the increase in the squareness of the magnetic hysteresis curve and coercivity. Thus, the results shown in Table 4 indicate that the applied magnetic field increased the magnetic anisotropy within the bulk magnet, showing increases of 5% in M_r/M_s, 2% in coercivity, and 9% in BH_{max} compared to the sample printed in the absence of a magnetic field. Compared to other samples manufactured by applying a magnetic field during MEX, M_r/M_s increased by approximately 16% when a magnetic field of 148–216 mT was applied. In the samples used in this study, a 5% improvement in M_r/M_s was observed when a magnetic field more than 10 times smaller (10 mT) was applied, indicating that even small magnetic fields of 10~15 mT are effective in increasing magnetic anisotropy. The sample that was applied with a 125 mT magnetic field for 15 min significantly increased magnetic properties, showing that it is important to increase the magnetic field application time. Therefore, the nozzle design of this study, with an extended range of magnetic field application, is suitable for improving magnetic alignment.

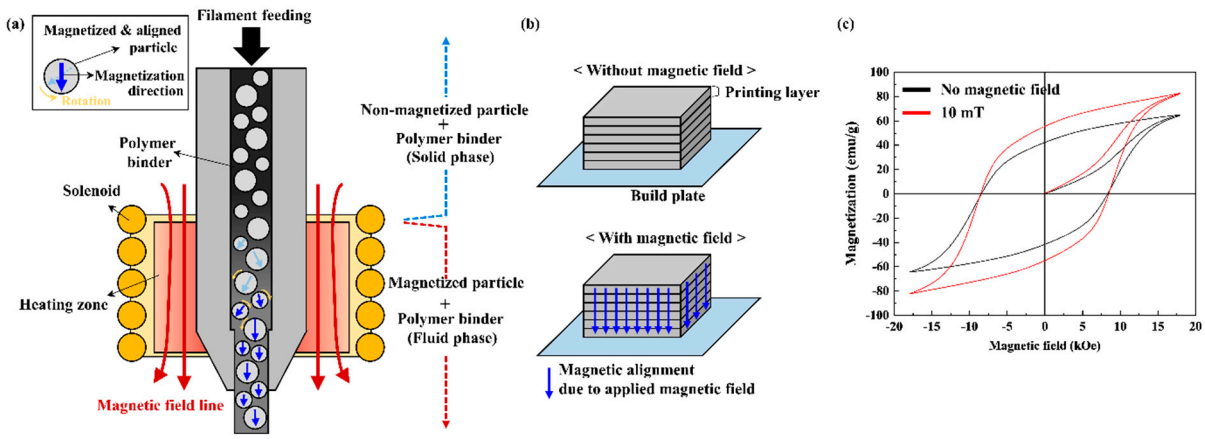

Figure 8. (**a**) Magnetic alignment process of magnetic particles in the filament under a magnetic field during MEX, (**b**) main magnetic alignment direction of the as-printed sample with or without magnetic field application, and (**c**) magnetic hysteresis curves according to the magnetic field.

Table 4. Magnetic properties of the bonded magnet according to the magnetic field.

Materials	Manufacturing Method	Magnetic Field (mT)	Magnetic Properties					
			Initial Slope (emu/gOe)	Coercivity (Oe)	BHmax (kGOe)	Saturation Magnetization (emu/g)	Remanence (emu/g)	Mr/Ms
This study NdFeB +PA12	MEX process under magnetic fields	0	1.92	8305	853	65	42	0.64
		10	2.72	8496	931	83	55	0.67
[25] NdFeB/SmFeN +PA12	MEX process under magnetic fields	0	-	12,600	-	-	-	0.55
		148–216	-	12,000	-	-	-	0.64
[27] NdFeB +PA12	Heating the manufactured bonded magnet for 15 min under magnetic fields	0	-	12,750	1750	-	-	0.48
		125	-	13,600	4000	-	-	0.70

Table 5 presents a summary of the magnetic field strength and temperature conditions for the magnetic alignment of bonded magnets reported in previous studies. For instance, Kim et al. [28] used ink-containing Nd-Fe-B powder and reported on the printing of structures capable of shape deformation by controlling magnetic alignment. They reported that magnetic alignment is possible even in a small magnetic field of 20 mT. In contrast, the magnetic field applied during printing in this study is only 10 mT, which is weaker than the magnetic field strength used in previous research. However, the magnetic property analysis results indicated that magnetic alignment occurred even in a small magnetic field (10 mT) when the binder melted and sufficient flow was secured. The mechanism for magnetic alignment occurring in such a small magnetic field is explained below.

Table 5. Magnetic field strength and temperature for the magnetic alignment of bonded magnets reported in previous studies.

Material		Magnetic Field (mT)	Temperature (°C)	Manufacturing Method	Ref.
Powder	Polymer Binder				
Anisotropic NdFeB alloy	Ethylene vinyl acetate	1000–5000	50–130	Heating the manufactured bonded magnet for 15 min under magnetic fields	[26]
Sm2Fe17N3	PA12	100–200	300	MEX process under a magnetic field	[21]
Sm2Fe17N3	PA12	90–100	260	MEX process under a magnetic field	[19]
Anisotropic NdFeB alloy	PA12	125–1000	220, 238, 256	Heating the manufactured bonded magnet for 15 min under magnetic fields	[27]
Anisotropic NdFeB alloy	Mixture of two Silicone-based materials	20–50	-	Ink-jet printing under a magnetic field	[28]
NdFeB/SmFeN alloy	PA12	90–216	180–300	MEX process under a magnetic field	[25]

During the MEX process, the magnetic particles are initially embedded within a solid polymer matrix, which limits their rotation. During this moment, the magnetic spins and domains in magnetic particles are preferentially aligned in the direction of the induced magnetic field. Subsequently, as the polymer melts and becomes a fluid from heating, the viscosity of the polymer decreases, enabling the magnetic particles to move more freely. Then, the external magnetic field can rotate the magnetic particles, precisely aligning their magnetization direction to the direction of the magnetic field. Under the sufficient magnetic field, the torques experienced by magnetic particles within the molten polymer matrix can be classified into three categories:

(1) Magnetic torque: This torque causes the rotation and alignment of magnetic particles under the influence of a magnetic field.
(2) Drag torque: This torque hinders the rotation of magnetic particles and depends on the relative angular velocity between the fluid phase and the magnetic particles.
(3) Particle-to-particle interaction torque: This torque is caused by the interaction between neighboring magnetic particles and can either support or oppose alignment, depending on the magnetic moment vectors of the particles. This interaction is called magnetostatic interaction.

The magnetic torque (τ_m), which causes the rotation and alignment of magnetic particles in a magnetic field, can be expressed for spherical particles in a magnetic field as follows:

$$\tau_m = m \times H = M\forall|H|\sin(\theta_P)(\hat{m} \times \hat{H}) \quad (3)$$

where M is the magnetization of the particle, $\forall$ is the particle volume, H is the magnetic field strength, θ_P is the particle magnetization angle with respect to the magnetic field direction, and $m = M\forall\hat{m}$ is the magnetic moment of the particle.

The magnetic particles in the molten filament can be precisely aligned with magnetic torque caused by an external magnetic field, which increases the magnetic anisotropy of the permanent magnet and enhances hard magnetic properties such as coercivity, remanence, and BH_{max}. However, the viscosity and friction of the molten filament produce a torque that opposes the magnetic torque induced by the applied magnetic field. To overcome this resistance, a sufficient external magnetic field is required to align the magnetic particles in the direction of the field. Bonded magnets have a polymer binder between the magnetic

particles, which can be viewed as a distribution of non-interacting magnetic particles separated by a non-magnetic polymer binder. As the temperature increases, the viscosity of the binder decreases, and the magnetostatic interaction between the particles becomes stronger. This eventually enables the magnetic particles to move, increasing the magnetic interaction between them. Therefore, the nozzle temperature and viscosity of the binder are critical factors in achieving magnetic alignment. Depending on the nozzle temperature and binder viscosity, magnetic alignment can be achieved when the applied magnetic field overcomes the magnetostatic interaction between magnetic particles and the rotation resistance to magnetic particles due to the binder [27].

In this study, the magnetic particles in the filament have various sizes and are separated by a polymer binder containing approximately 70 vol%. Consequently, the magnetic particles are isolated because of the binder, making it challenging for their distribution to change significantly in the applied 10 mT magnetic field. Therefore, the magnetic interaction between the particles is small, enabling them to overcome the magnetostatic interaction. Furthermore, the reduced viscosity of the binder at the high printing temperature enables the rotation of the magnetic particles, effectively increasing magnetic anisotropy.

The application of the magnetic field in the AM process enhances the magnetic anisotropy of bonded magnets. Magnetic alignments were achieved even in smaller magnetic fields owing to the fluid-phase binder. This study demonstrated that the high geometric freedom provided by AM enables the production of bonded magnets with shapes that were previously impossible to achieve. We anticipate that the high geometric freedom provided by AM will enable the implementation of strategies to enhance the magnetic properties of bonded magnets in terms of design, such as segment magnets. However, beyond the manufacturing of bonded magnets having magnetic anisotropy, additional research is required to develop the in situ magnetic field-applied MEX process into a production technology for manufacturing bonded magnets with improved magnetic properties. Consequently, the development and manufacturing of spherical magnetic powder with strong magnetocrystalline anisotropy are preferentially required. Moreover, further research is required on the influence of magnetic field strength on hard magnetic properties.

4. Conclusions

In conclusion, this study introduced an MEX nozzle equipped with an in situ magnetic field application system to manufacture bonded magnets with in situ magnetic alignment. The MEX nozzle was optimized to generate a magnetic field using a solenoid that rotates the magnetic particles when the polymer binders are in a liquid phase, resulting in a magnetic alignment effect. This solenoid was integrated into the melting zone of the nozzle. The magnetic field strength was measured at 10 mT at the bottom of the solenoid, and it was predicted to be approximately 15 mT internally. Moreover, the results demonstrated that using the developed nozzle, bonded magnets were produced with improved magnetic properties, such as remanence, coercivity, and maximum energy product, when a magnetic field was applied, confirming the increase in magnetic anisotropy due to magnetic alignment. The proposed MEX nozzle with a magnetic field application system is expected to facilitate the production of complex-shaped bonded magnets with improved magnetic properties without molds. Bonded magnets can be produced economically while simultaneously achieving the realization of complex 3D shapes and the improvement of magnetic properties in a single process step through the proposed MEX nozzle. As it becomes possible to manufacture bonded magnets of various shapes considering magnetic properties, the performance of components can be improved in terms of magnet designs. The MEX process using a nozzle with a magnetic field application system can be used to manufacture bonded magnets for various electrical devices such as sensors, motors, and actuators. Further research is required to investigate the influence of the magnetic field strength, printing conditions, and applied materials on magnetic alignment, which will assist in the development of more effective manufacturing methods for bonded magnets.

Author Contributions: Conceptualization, H.Y.J. and J.Y.H.; methodology, J.Y.H. and H.Y.J.; software, S.J.P. and Y.S.; validation, H.Y.J. and J.Y.H.; formal analysis, J.Y.H. and S.J.P.; investigation, J.Y.H.; resources, H.Y.J. and Y.S.; data curation, J.Y.H.; writing—original draft preparation, J.Y.H.; writing—review and editing, J.Y.H. and H.Y.J.; visualization, J.Y.H.; supervision, H.Y.J.; project administration, H.Y.J.; funding acquisition, H.Y.J. All authors have read and agreed to the published version of the manuscript.

Funding: This research was funded by the Korea Institute of Industrial Technology (PEH23084).

Data Availability Statement: Some data in this article was reported in annual project report of Korea Institute of Industrial Technology (PEM22130).

Conflicts of Interest: The authors declare no conflict of interest.

References

1. Pigliaru, L.; Paleari, L.; Bragaglia, M.; Nanni, F.; Ghidini, T.; Rinaldi, M. Poly-ether-ether-ketone—Neodymium-iron-boron bonded permanent magnets via fused filament fabrication. *Synth. Met.* **2021**, *279*, 116857. [CrossRef]
2. Cao, Y.; Zhu, M.; Rong, M.Z.; Zhang, M.Q. Injection moldable, self-healable, and recyclable rubber-bonded NdFeB magnets with the magnetic particulates content up to 90 wt%. *Adv. Compos.* **2023**, *6*, 38. [CrossRef]
3. Qu, Z.; Wu, Q.; Zhang, M.; Yue, M.; Liu, W. Facile preparation of bonded NdFeB/SmFeN hybrid magnets with flexibility, anisotropy and high energy density. *J. Magn. Magn. Mater.* **2023**, *584*, 171084. [CrossRef]
4. Mungale, K.; Lamichhane, T.N.; Wang, H.; Sales, B.C.; Paranthaman, M.P.; Vaidya, U.K. Compression molding of anisotropic NdFeB bonded magnets in a polycarbonate matrix. *Materials* **2021**, *19*, 101167.
5. Magnet Manufacturing Process. Available online: https://www.arnoldmagnetics.com/resources/magnet-manufacturing-process/ (accessed on 21 September 2023).
6. Injection Molded Magnet. Available online: https://www.magnet-sdm.com/injection-molded-magnet/ (accessed on 21 September 2023).
7. Li, L.; Jones, K.; Sales, B.; Pries, J.L.; Nlebedim, I.C.; Jin, K.; Bei, H.; Post, B.K.; Kesler, M.S.; Rios, O.; et al. Fabrication of highly dense isotropic Nd-Fe-B nylon bonded magnets via extrusion-based additive manufacturing. *Addit. Manuf.* **2018**, *21*, 495–500. [CrossRef]
8. Petersdorff-Campen, K.; Hauswirth, Y.; Carpenter, J.; Hagmann, A.; Boës, S.; Daners, M.S.; Penner, D.; Meboldt, M. 3D printing of functional assemblies with integrated polymer-bonded magnets demonstrated with a prototype of a rotary blood pump. *Appl. Sci.* **2018**, *8*, 1275. [CrossRef]
9. Slapnik, J.; Pulko, I.; Rudolf, R.; Anžel, I.; Brunčko, M. Fused filament fabrication of Nd-Fe-B bonded magnets: Comparison of PA12 and TPU matrices. *Addit. Manuf.* **2021**, *38*, 101745. [CrossRef]
10. Li, L.; Tirado, A.; Nlebedim, I.C.; Rios, O.; Post, B.; Kunc, V.; Lowden, R.R.; Lara-Curzio, E.; Fredette, R.; Ormerod, J.; et al. Big area additive manufacturing of high performance bonded NdFeB magnets. *Sci. Rep.* **2016**, *6*, 36212. [CrossRef]
11. Paranthaman, M.P.; Yildirim, V.; Lamichhane, T.N.; Begley, B.A.; Post, B.K.; Hassen, A.A.; Sales, B.C.; Gandha, K.; Nlebedim, I.C. Additive manufacturing of isotropic NdFeB PPS bonded permanent magnets. *Materials* **2020**, *13*, 3319. [CrossRef]
12. Huber, C.; Abert, C.; Bruckner, F.; Groenefeld, M.; Muthsam, O.; Schuschnigg, S.; Sirak, K.; Thanhoffer, R.; Teliban, I.; Vogler, C.; et al. 3D print of polymer bonded rare-earth magnets, and 3D magnetic field scanning with an end-user 3D printer. *Appl. Phys. Lett.* **2016**, *109*, 162401. [CrossRef]
13. Azimi, G.; Sauber, M.E.; Zhang, J. Technoeconomic analysis of supercritical fluid extraction process for recycling rare earth elements from neodymium iron boron magnets and fluorescent lamp phosphors. *J. Clean. Prod.* **2023**, *422*, 138526. [CrossRef]
14. Delette, G. $Nd_2Fe_{14}B$ permanent magnets substituted with non-critical light rare earth elements (Ce, La): A review. *J. Magn. Magn. Mater.* **2023**, *577*, 170768. [CrossRef]
15. An, S.; Ma, Z.; Li, W.; Zhang, H.; Yin, T. Magnetic properties of anisotropic bonded NdFeB/SmCo permanent magnets. *AIP Adv.* **2019**, *9*, 125146. [CrossRef]
16. Gao, R.W.; Zhang, J.C.; Zhang, D.H.; Dai, Y.Y.; Meng, X.H.; Wang, Z.M.; Zhang, Y.J.; Liu, H.Q. Dependence of the magnetic properties on the alignment magnetic field for NdFeB bonded magnets made from anisotropic HDDR powders. *J. Magn. Magn. Mater.* **1999**, *191*, 97–100. [CrossRef]
17. Wang, H.; Lamichhane, T.N.; Paranthaman, M.P. Review of additive manufacturing of permanent magnets for electrical machines: A prospective on wind turbine. *Mater. Today Phys.* **2022**, *24*, 100675. [CrossRef]
18. Gandha, K.; Li, L.; Nlebedim, I.C.; Post, B.K.; Kunc, V.; Sales, B.C.; Bell, J.; Paranthaman, M.P. Additive manufacturing of anisotropic hybrid NdFeB-SmFeN nylon composite bonded magnets. *J. Magn. Magn. Mater.* **2018**, *467*, 8–13. [CrossRef]
19. Suppan, M.; Huber, C.; Mathauer, K.; Abert, C.; Brucker, F.; Gonzalez-Gutierrez, J.; Schuschnigg, S.; Groenefeld, M.; Teliban, I.; Kobe, S.; et al. In situ alignment of 3D printed anisotropic hard magnets. *Sci. Rep.* **2022**, *12*, 17590. [CrossRef]
20. Sarkar, A.; Paranthaman, M.P.; Nlebedim, I.C. In-situ magnetic alignment model for additive manufacturing of anisotropic bonded magnets. *Addit. Manuf.* **2021**, *46*, 102096. [CrossRef]

21. Sonnleitner, K.; Huber, C.; Teliban, I.; Kobe, S.; Saje, B.; Kagerbauer, D.; Reissner, M.; Lengauer, C.; Groenefeld, M.; Suess, D. 3D printing of polymer-bonded anisotropic magnets in an external magnetic field and by a modified production process. *Appl. Phys. Lett.* **2020**, *116*, 092403. [CrossRef]
22. Nagarajan, B.; Aguilera, A.F.E.; Wiechmann, M.; Qureshi, A.J.; Mertiny, P. Characterization of magnetic particle alignment in photosensitive polymer resin: A preliminary study for additive manufacturing processes. *Addit. Manuf.* **2018**, *22*, 528–536. [CrossRef]
23. Jung, H.Y.; Choi, K.S.; Hwang, J.Y. Nozzle Assembly, Three-Dimensional Printer and Three-Dimensional Printing Method Including the Same, and Electronic Component Case Manufactured Using the Same. International Patent System PCT/KR2022/019041, 29 November 2022.
24. Park, S.J.; Lee, J.E.; Park, J.Y.; Lee, N.K.; Son, Y.; Park, S.H. High-temperature 3D printing of polyetheretherketone products: Perspective on industrial manufacturing applications of super engineering plastics. *Mater. Des.* **2021**, *211*, 110163. [CrossRef]
25. Sarkara, A.; Somashekara, M.A.; Paranthaman, M.P.; Kramer, M.; Haase, C.; Nlebedim, I.C. Functionalizing magnet additive manufacturing with in-situ magnetic field source. *Addit. Manuf.* **2020**, *34*, 101289. [CrossRef]
26. Nlebedim, I.C.; Ucar, H.; Hatter, C.B.; McCallum, R.W.; McCall, S.K.; Kramer, M.J.; Paranthaman, M.P. Studies on in situ magnetic alignment of bonded anisotropic Nd-Fe-B alloy powders. *J. Magn. Magn. Mater.* **2017**, *422*, 168–173. [CrossRef]
27. Khazdozian, H.A.; Li, L.; Paranthaman, M.P.; McCall, S.K.; Kramer, M.J.; Nlebedim, I.C. Low-field alignment of anisotropic bonded magnets for additive manufacturing of permanent magnet motors. *JOM* **2019**, *71*, 626–632. [CrossRef]
28. Kim, Y.H.; Yuk, H.W.; Zhao, R.; Chester, S.A.; Zhao, X. Printing ferromagnetic domains for untethered fast-transforming soft materials. *Nature* **2018**, *558*, 274–279. [CrossRef]